

## Improvement of $\text{Pb}(\text{Zr}_{0.52}\text{Ti}_{0.48})\text{O}_3$ Thin Films with $\text{LaNiO}_3$ as Bottom Electrodes

T.J. Zhu<sup>1</sup> and Li Lu<sup>1,2</sup>

<sup>1</sup> Singapore-MIT Alliance, National University of Singapore, 4 Engineering Drive 3, Singapore 117576

Fax: 65-68742241, e-mail: smazhutj@nus.edu.sg

<sup>2</sup> Department of Mechanical Engineering, National University of Singapore, 9 Engineering Drive 1, Singapore 117576

Fax: 65-67791459, e-mail: mpeluli@nus.edu.sg

$\text{Pb}(\text{Zr}_{0.52}\text{Ti}_{0.48})\text{O}_3$  (PZT) ferroelectric thin films have been deposited on Pt/Ti/SiO<sub>2</sub>/Si and single crystal bare Si substrates with or without  $\text{LaNiO}_3$  (LNO) bottom electrodes by pulsed laser deposition. X-ray diffraction (XRD) revealed the presence of pyrochlore phase when PZT thin films were deposited directly on Pt/Ti/SiO<sub>2</sub>/Si substrates, while complete ferroelectric perovskite phases were obtained for PZT thin films on LNO/Pt/Ti/SiO<sub>2</sub>/Si and LNO/Si substrates. The full perovskite PZT polycrystalline films with LNO as bottom electrodes exhibit rosette-like structure, different from the fine-grained structure of the PZT films on Pt/Ti/SiO<sub>2</sub>/Si substrates. Polarization – Electric field hysteresis loop measurement demonstrates that the PZT thin film with LNO/Pt double electrode possesses highest remnant polarization and coercive field, about 13 $\mu\text{C}/\text{cm}^2$  and 87kV/cm, respectively. The depth profile of a PZT/LNO/Pt/Ti/SiO<sub>2</sub>/Si multilayer structure performed by Secondary Ion Mass Spectroscopy shows that no marked diffusion occurred at the PZT/LNO interface. The present work reveals that LNO thin film is an excellent conductive oxide electrode and a suitable seeding layer for perovskite PZT thin films.

**Keywords:** Lead zirconate titanate, thin films, pulsed laser deposition, bottom electrodes.

### 1. INTRODUCTION

Ferroelectric oxide thin films have attracted considerable attention for a variety of applications in ferroelectric memories, piezoelectric micro-actuators and sensors, optoelectronic devices and pyroelectric detectors [1, 2]. Among many types of ferroelectric materials, the lead zirconate titanate (PZT) family of perovskites and its derivatives are being intensively investigated in recent years. They have been grown on various substrates, such as Si, SrTiO<sub>3</sub> (STO), MgO and LaAlO<sub>3</sub> (LAO), to study the role of crystalline quality on electrical properties [3-5]. Polycrystalline ferroelectric thin films are conventionally grown on Pt-coated Si substrates with Pt top contact electrodes to form the metal-insulator-metal (MIM) capacitor structure because Pt has good metallic properties and high oxidation resistance [6-8]. However, the high-angle grain boundaries in ferroelectric thin films and poor interfaces between the ferroelectric layer and metal electrode deteriorate device performance. Moreover pyrochlore phase can be frequently observed in PZT films even though PZT targets contain excess amount of lead oxide and high oxygen pressure during deposition are used to overcome the loss of Pb. Hence conducting oxide electrodes with perovskite structure have been developed to surmount the above problems [9].

PZT films with superior properties have been successfully obtained with YBa<sub>2</sub>Cu<sub>3</sub>O<sub>7</sub> (YBCO), SrRuO<sub>3</sub> (SRO) and (La,Sr)CoO<sub>3</sub> (LSCO) as bottom electrodes [9]. However, YBCO superconductor has not been seriously considered as a suitable electrode for integrated ferroelectric capacitors because of its low

chemical stability and poor surface roughness [10]. The presence of outgrowths in a SRO film will also limit its application as electrodes [11].  $\text{LaNiO}_3$  (LNO) is an isotropic n-type metallic oxide with low resistivity of about 150-210 $\mu\Omega$  cm at 300K comparable to that of LSCO but simpler composition than LSCO. Since it also has a perovskite structure with a lattice constant of 0.386nm well matching with that of PZT, it can promote oriented and even epitaxial growth of PZT thin films [5].

In this work, PZT thin films were comparatively deposited on LNO and Pt coated Si substrates by pulsed laser deposition technique, with particular emphasis on how the LNO single layer and the LNO/Pt double layer electrode improve the microstructures and properties of these ferroelectric films.

### 2. EXPERIMENTAL PROCEDURES

Pulsed laser deposition (PLD) method was used to fabricate PZT and LNO films. A Lambda Physik KrF excimer laser beam ( $\lambda = 248\text{nm}$ , pulse width = 25ns) was incident on the rotating target at an angle of about 45°. The target-substrate distance was kept at 45mm. The chamber was evacuated to a base pressure less than  $2 \times 10^{-5}$  Torr.

The Pt/Ti/SiO<sub>2</sub>/Si(100) and bare Si(100) substrates were cleaned in organic solvent baths in an ultrasonic container. Bare Si substrates were dipped in 20% HF solution for 2 minutes to remove surface native oxide prior to loading into the chamber. The commercial LNO target was stoichiometric with purity of about 99.9%. The PZT target was fabricated by conventional solid state reaction with a composition corresponding to Zr/Ti

ratio of 0.52/0.48. The laser ablation was carried out at a laser fluence of 2-5 J/cm<sup>2</sup> and a repetition rate of 10Hz. The LNO films were deposited at the substrate temperatures of 580°C and the oxygen partial pressures of 50mTorr, whereas the deposition of PZT was controlled at 600°C and 400 mTorr.

Structure and crystallinity of the thin film samples were measured using a Shimadzu XRD-6000 X-ray diffractometer (XRD) with Cu K $\alpha$  radiation. Surface morphology of the thin films was characterized using a Digital Instrument Dimension 3100 atomic force microscopy (AFM) operated in the tapping mode. The depth profiles of the PZT capacitors were performed by a Cameca IMS 6f secondary ion mass spectroscopy (SIMS) using 12.5 keV O<sub>2</sub><sup>+</sup> as a primary ion source. The ion beam was raster-scanned across a square of 250 × 250 μm<sup>2</sup> on the sample and a detection circular area with a diameter of 60 μm in the center was used to avoid crater-edge effects. To measure the electrical properties, Pt electrodes of 500μm diameter were deposited through a shadow mask onto the top of PZT films by sputtering to serve as the top electrodes. Ferroelectric hysteresis behavior was studied using a Precision Workstation Materials Analyzer (Radiant Technologies, USA).

### 3. RESULTS AND DISCUSSION

Fig.1 shows the XRD spectra of the PZT films fabricated on the various substrates. As can be seen, the XRD spectrum of the PZT film deposited on the Pt/Ti/SiO<sub>2</sub>/Si substrate reveals a (222) diffraction peak of pyrochlore phase at about 29.6° in addition to the diffraction peaks of main perovskite PZT and Pt electrode, indicating the formation of perovskite-pyrochlore mixed structure. The result is in agreement with previous studies [12, 13].

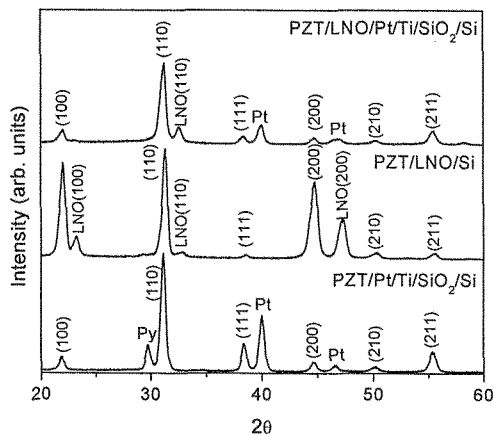


Fig.1. XRD spectra of the PZT films fabricated on Pt/Ti/SiO<sub>2</sub>/Si, LNO/Si and LNO/Pt/Ti/SiO<sub>2</sub>/Si substrates.

For the PZT/LNO/Si heterostructure, the (100) and (200) diffractions of the LNO pseudocubic structure were observed with the weak (110) peak, indicating the formation of the preferentially (100)-textured LNO film. All peaks identified for the PZT film come from the perovskite phase without the presence of pyrochlore phase. The ratio of the intensity of the PZT(100) to (110) peaks was measured to be 87:100. Comparing to the value of 12:100 (JCPDS No. 33-0784) for a randomly oriented PZT powder sample, it was found that the fully

perovskite structure with preferred (100)-texture to certain degree was formed on the (100)-textured LNO film. Such a phenomenon is associated to the similarity in crystal structure and lattice parameters between the LNO and PZT materials.

As shown in Fig.1 (upper pattern), the LNO film on the Pt coated substrate preferentially orients in the <110> direction and the XRD spectrum of the PZT film deposited on the LNO/Pt/Ti/SiO<sub>2</sub>/Si(100) substrate reveals complete perovskite structure, which further confirms that LNO film is a suitable template for facilitating the growth of perovskite PZT films. However, it was observed that the ratio of the intensity of PZT(100) to (110) peak decreases to 18:100 in comparison with the PZT film grown on the LNO/Si substrate. The above results demonstrate that the use of LNO films not only promote the formation of complete perovskite PZT films, but their orientations will also influence those of PZT overlayers.

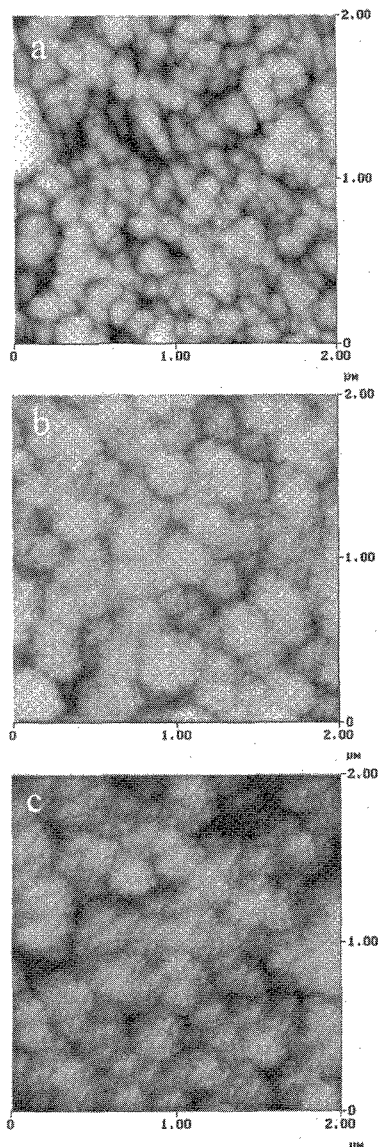


Fig.2. AFM images of the surface topography of the PZT films deposited on: (a) Pt/Ti/SiO<sub>2</sub>/Si, (b) LNO/Si and (c) LNO/Pt/Ti/SiO<sub>2</sub>/Si substrates.

Typical AFM images at  $2 \times 2 \mu\text{m}$  scale of the surface topography of the PZT films deposited on the various substrates are shown in Fig.2. No cracks except for laser-induced droplets can be observed on the surface of these PZT films. As shown in Fig. 2 (a), the PZT film deposited on the Pt/Ti/SiO<sub>2</sub>/Si substrate reveals relatively homogeneous and fine-grained surface morphology, while the morphology of the PZT film on the LNO/Si substrate, as shown in Fig. 2(b), is different, exhibiting a rosette-like feature that is often seen on PZT films annealed at high temperatures [14, 15]. The rosette structure is generally attributed to the perovskite PZT phase, whereas the fine-grained morphology is believed to consist of Pb-deficient pyrochlore phase, PbTi<sub>3</sub>O<sub>7</sub> or Pb<sub>2</sub>Ti<sub>2</sub>O<sub>6+x</sub> [15], which is in good agreement with XRD spectra shown in Fig.1. A circular morphology is observed for isolated rosettes and each rosette is an assembly of the close-packed round grains at nanometer scale. These grains are finer than those in the PZT film on the Pt/Ti/SiO<sub>2</sub>/Si substrate. The surface morphology of the PZT film on the LNO/Pt/Ti/SiO<sub>2</sub>/Si substrate as shown in Fig. 2 (c) is similar to that of the PZT film on the LNO/Si. The root-mean-square (rms) roughness of the randomly selected regions is 20.0, 16.5 and 13.6nm for the PZT films on the Pt/Ti/SiO<sub>2</sub>/Si, LNO/Si, LNO/Pt/Ti/SiO<sub>2</sub>/Si substrates, respectively. The large rms surface roughness results from the island growth mechanism (Volmer-Weber mode) of these PZT films, which can be reasonably deduced from the AFM images shown in Fig.2.

Fig.3 shows the *P-E* ferroelectric hysteresis loops at a frequency of 1kHz and triangular pulses of  $\pm 3$ ,  $\pm 4$ ,  $\pm 5$ V for the PZT films of 200nm thickness. As shown in Fig. 3(a), the remnant polarization and coercive field increase with increasing peak voltage and saturates at approximate 5V peak voltage. The remnant polarization  $P_r$  and the coercive field  $E_c$  at 5V, which are averaged with the positive and negative values, are estimated to be  $6\mu\text{C}/\text{cm}^2$  and  $85\text{kV}/\text{cm}$ , respectively. The presence of pyrochlore phase in the film is detrimental to ferroelectric properties. For the Pt/PZT/LNO capacitor structure shown in Fig. 3 (b), it is noted that the hysteresis loop reveals marked asymmetry and the loop shifts to the positive direction of the electric field axis. If the polarization is reversed by applying a positive field to the Pt top electrode, the extra quantity as much as the internal field is required compared to the coercive field of the symmetric hysteresis loop. The internal field is believed to result from the interface effects and the asymmetric distribution of space charges along the normal of the film surface, and it is estimated to be  $22.5\text{kV}/\text{cm}$  for the present work. The averaged remnant polarization and coercive field at 5V for the Pt/PZT/LNO capacitor are about  $10\mu\text{C}/\text{cm}^2$  and  $77\text{kV}/\text{cm}$  respectively, which are superior over the Pt/PZT/Pt capacitor. This observation indicates LNO films are suitable electrode layer to improve ferroelectric properties of PZT films. However, one of drawbacks of using LNO as bottom electrodes is its high resistivity. An LNO/Pt double layer electrode was therefore used to improve the electrical properties of PZT capacitors due to the bypassing effect of the Pt layer and hence lower surface resistivity of electrode materials. The measured hysteresis loops are shown in Fig. 3 (c). The remnant

polarization and coercive field at 5V is  $13\mu\text{C}/\text{cm}^2$  and  $87\text{kV}/\text{cm}$ , respectively. The values are comparable with the results reported by Tseng et al.[16], who deposited PZT films on LNO/Pt coated Si<sub>3</sub>N<sub>4</sub>/Si substrates. The increase in the coercive field, compared to the PZT film with LNO single electrode, is attributed to the change in the microstructure because of the different orientations of the LNO underlayers, as shown in Fig. 1. It is noteworthy that the PZT/LNO/Pt capacitor has larger polarization value than the PZT/LNO one although the latter has relatively large degree of (100) orientation. One reason is due to the bypassing effect of the Pt layer, as mentioned above. The other is because in a tetragonal structure of perovskite PZT crystals maximum polarization is expected to occur in the  $\langle 001 \rangle$  direction not in the  $\langle 100 \rangle$  direction.

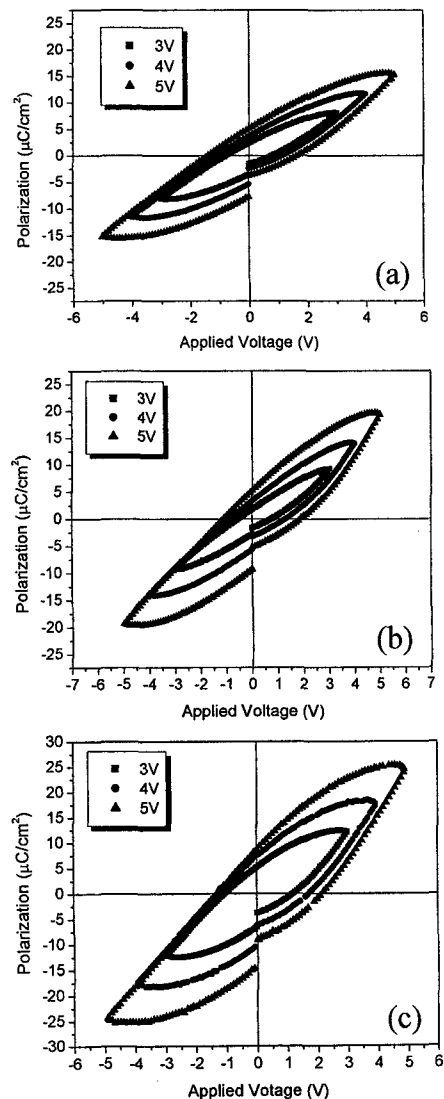


Fig.3. *P-E* ferroelectric hysteresis loops of PZT films on different underlayers: (a) Pt/PZT/Pt, (b) Pt/PZT/LNO and Pt/PZT/LNO/Pt capacitors at  $\pm 3$ ,  $\pm 4$  and  $\pm 5$ V.

The SIMS profile of the PZT film on LNO/Pt/Ti/SiO<sub>2</sub>/Si substrate is shown in Fig. 4. The ion count profiles of Pb, Zr and Ti indicate a homogeneous composition distribution in the PZT film along depth direction. No distinct interdiffusion at the PZT/LNO

interface can be found. The Ti layer pre-coated underneath the Pt layer for improving the adhesion of the overlayer diffused all the way through the Pt layer. The outward and inward diffusion of the La element is ignorable, while the Ni species inward diffused into Pt/Ti layers, implying Pt/Ti are not good barrier layers for LNO films. The unusually high  $^{90}Zr$  content in  $SiO_2/Si$  substrate is attributed to the  $^{30}Si^{30}Si^{30}Si$  interference. The increase of Pt and Pb ion counts in the PZT and Pt/Ti layers respectively cannot be understood at present, although it is suspected to result from signal interference or other effects.

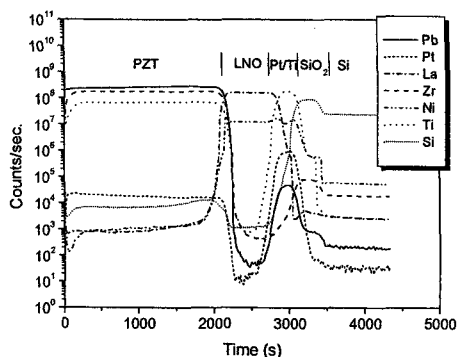


Fig.4. SIMS profile of the PZT film on LNO/Pt/Ti/SiO<sub>2</sub>/Si substrate.

#### 4. CONCLUSIONS

PZT thin films have been fabricated on Pt/Ti/SiO<sub>2</sub>/Si, LNO/Si, LNO/Pt/Ti/SiO<sub>2</sub>/Si substrates by pulsed laser deposition. It is found that LNO films not only facilitate the growth of full perovskite PZT films, but also improve electrical properties of the films. The use of LNO/Pt double layer electrodes can further increase the remnant polarization due to the bypassing effect of Pt layer. The full perovskite PZT films with LNO as bottom electrodes have a rosette-like microstructure, while the PZT films with a small amount of pyrochlore phase on Pt/Ti/SiO<sub>2</sub>/Si substrates reveal fine-grained structure. No significant interdiffusion can be observed at the PZT/LNO interface. It is believed that investigating the interaction between PZT films and substrates is the key to understand the role of intermediate layer such as LNO on the growth and electrical properties of PZT films.

#### ACKNOWLEDGEMENTS

This research was supported by Advanced Materials for Micro- and Nano-System (AMM&NS) program under Singapore-MIT Alliance (SMA) Program and by National University of Singapore. Authors would like to thank Professor Carl V. Thompson from the Department of Materials Science and Engineering, Massachusetts Institute of Technology, Cambridge for useful discussions.

#### REFERENCES:

1. J.F. Scott and C.A. Paz de Araujo, *Science*, **246**, 1400 (1989).
2. O. Auciello and R. Waser, eds. "Science and technology of electroceramic thin films", Kluwer Academic, Boston (1995).
3. R. Ramesh, A. Inam, W. K. Chan, F. Tillerot, B. Willens, C. C. Chang, T. Scands, J. M. Tarascon, and

- V. G. Keramidis, *Appl. Phys. Lett.*, **59**(27), 3542 (1991).
4. W.M. Gilmore III, S. Chattopadhyay, A. Kvit, A.K. Sharma, C.B. Lee, W.J. Collis, J. Sankar, and J. Narayan, *J. Mater. Res.*, **18**(1), 111 (2003).
5. W. Wu, K.H. Wong, and C.L. Choy, *J. Vac. Sci. Technol.*, **A18** (1), 79 (2000).
6. M. Sayer and K. Sreenivas, *Science*, **247**, 1056 (1990).
7. T. Kumazawa, *Appl. Phys. Lett.*, **72**, 608 (1998).
8. L. H. Chang and W.A. Anderson, *Thin Solid Films*, **303**, 94 (1997).
9. R. Ramesh, S. Aggarwal, and O. Auciello, *Mater. Sci. Eng.*, **R 32**, 191 (2001).
10. L. Li, *Mater. Sci. Eng.*, **R 29**, 153 (2000).
11. J. Roldan, F. Sanchez, V. Trtik, C. Guerrero, F. Benitez, C. Ferrater, and M. Varela, *Appl. Surf. Sci.*, **154-155**, 159 (2000).
12. J. S. Horwitz, K.S. Grabowski, D.B. Chrisey, and R.E. Leuchtner, *Appl. Phys. Lett.*, **59**, 1565 (1991).
13. Y.C. Ling, J.P. Wang, M.H. Yeh, K.S. Liu, and I.N. Lin, *Appl. Phys. Lett.*, **66**(2), 156 (1995).
14. A.H. Carim, B.A. Tuttle, D.H. Doughty, and S.L. Martinez, *J. Am. Ceram. Soc.*, **74**, 1455 (1991).
15. K.S. Hwang, T. Manabe, T. Nagahama, I. Yamaguchi, T. Kumagai, and S. Mizuta, *Thin Solid Films*, **347**, 106 (1999).
16. T.-F. Tseng, R.-P. Yang, and K.-S. Liu, *Appl. Phys. Lett.*, **70**, 46 (1996).

(Received October 13, 2003; Accepted July 1, 2004)